ACS Medicinal Chemistry Letters

pubs.acs.org/acsmedchemlett Letter

Flavonol-Based Carbon Monoxide Delivery Molecule with Endoplasmic Reticulum, Mitochondria, And Lysosome Localization

Livia S. Lazarus, C. Taylor Dederich, Stephen N. Anderson, Abby D. Benninghoff, and Lisa M. Berreau*

Cite This: ACS Med. Chem. Lett. 2022, 13, 236−242 Read Online

ACCESS | Metrics & More | Article Recommendations | Supporting Information

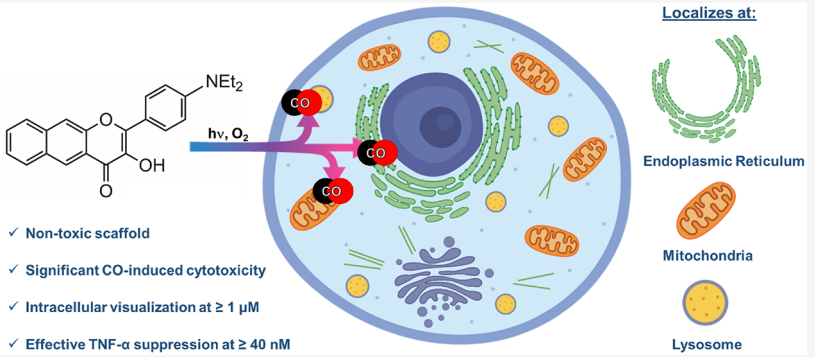

ABSTRACT: Light-triggered carbon monoxide (CO) delivery molecules are of significant current interest for evaluating the role of CO in biology and as potential therapeutics. Herein we report the first example of a metal free CO delivery molecule that can be tracked via confocal microscopy at low micromolar concentrations in cells prior to CO release. The NEt_2-appended extended flavonol (**4**) localizes to the endoplasmic reticulum, mitochondria, and lysosomes. Subcellular localization of **4** results in CO-induced toxicity effects that are distinct as compared to a nonlocalized analog. Anti-inflammatory effects of **4**, as measured by TNF-α suppression, occur at the nanomolar level in the absence of CO release, and are enhanced with visible-light-induced CO release. Overall, the highly trackable nature of **4** enables studies of the biological effects of both a localized flavonol and CO release at low micromolar to nanomolar concentrations.

KEYWORDS: *signaling, gasotransmitter, metal-free, aminoflavonol, cytotoxicity*

Known for centuries for its toxicity, carbon monoxide (CO) is of considerable current interest with regard to its role in biological signaling and as a potential therapeutic.[1,2] Produced endogenously in humans via the oxidative catabolism of heme,[3−6] CO is known to produce anti-inflammatory, antiapoptotic, antihypertensive, vasodialation, and cytoprotective effects.[7] Delivery of controlled amounts of CO is also known to produce antibacterial and anticancer effects.[8,9] On this basis, CO is of significant current interest for several biomedical applications.[10,11]

Heme oxygenases (e.g., HO-1) catalyze the O_2-dependent CO release from heme (Scheme 1a). The subcellular distribution of HO-1 is dynamic and is regulated by cellular homeostasis.[12] Under normal cell conditions, HO-1 is as a cytosol-facing endoplasmic reticulum (ER)-associated protein.[12] Under stress, HO-1 translocates in part to mitochondria, nucleus, and caveolae.[13] This stress-dependent distribution raises intriguing questions about how the intracellular location of CO release impacts its signaling effects.

As an approach toward investigating the biological roles of CO and its potential as a therapeutic agent, carbon monoxide releasing molecules (CORMs) were developed.[7,14,15] Although a significant body of CO research has been reported using metal−carbonyl-based CORMs, other biological activities of these complexes have also been identified.[16−18] The most commonly used metal carbonyl CORMs for biological studies, CORM-2 and CORM-3, release CO spontaneously in buffer and thus do not offer the possibility of examining the effects of localized intracellular CO delivery.[19,20]

Several laboratories are pursuing the development of metal-free CO delivery molecules.[21−33] The frameworks receiving the greatest attention for potential biomedical applications are norborn-2-ene-7-one derivatives developed by Wang and co-workers[27] and extended flavonols developed in our laboratory.[23,31] Although the former exhibit spontaneous CO release, the rates of which can be tuned via structural modifications,[33]

Received: October 26, 2021
Accepted: January 26, 2022
Published: February 1, 2022

https://doi.org/10.1021/acsmedchemlett.1c00595
ACS Med. Chem. Lett. 2022, 13, 236−242

Scheme 1. CO Release Reactions of (a) Heme Oxygenase and (b) 1

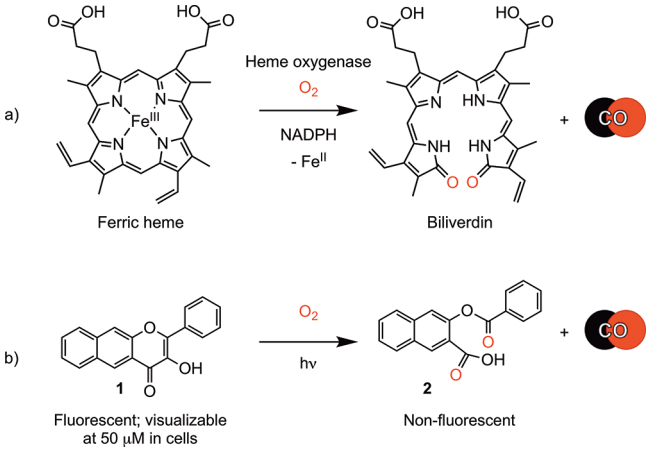

CO release from extended flavonols is triggered using visible light. The flavonols thus offer the possibility of highly controlled and localized CO release, including when delivered as part of micelles, materials, or polymers.[8,34−38]

We have previously reported that **1** (Scheme 1b) undergoes visible-light-induced CO release to give **2**.[23] Compound **1** is fluorescent, whereas **2** is nonemissive. These attributes enable fluorescence tracking of **1** in A549 cells prior to CO release.[23] A concentration of 50 μM or higher is needed for visualization of **1** in cells as its emission rapidly bleaches upon illumination. This behavior has thus far prevented studies of **1** using confocal microscopy. The fluorescence microscopy studies of **1** suggest dispersion throughout the cytoplasm.

The development of molecules for localized intracellular CO delivery remains in its very early stages. Wang has reported a bio-orthogonal reaction-based pair of compounds that are localized to mitochondria via phosphonium appendages.[39] A fluorescent fluoranthene product provides evidence for localized CO release in this system. A phosphonium-appended, mitochondria-targeting extended flavonol (**3**, Scheme 2) is trackable via its emission prior to visible-light-induced CO release.[40] This localized delivery of CO from **3** (at 10 μM) produces decreases in mitochondrial basal respiration, ATP production, maximal respiration, and reserve capacity. The observed changes are similar to those found for cytosolic **1**, indicating that at a concentration of 10 μM, localized CO delivery to mitochondria does not produce differentiating effects on function. However, there are differences in the toxicity of the compounds, with **3** being more toxic in A549 cells (IC_{50} = 14.1 ± 2.7 μM) than **1** (IC_{50} = 80.2 ± 3.3 μM). With visible-light-driven CO release, **3** shows a mild increase in toxicity (IC_{50} = 4.6 ± 3.6 μM), whereas no change in toxicity occurs with CO delivery from **1** (IC_{50} = 76.1 ± 5.2 μM). The organic byproducts produced in the CO release reactions of **1** and **3** are both nontoxic up to 100 μM.

Scheme 2. (Top) Mitochondria-Targeting 3; (Bottom) CO-Release Reaction of 4

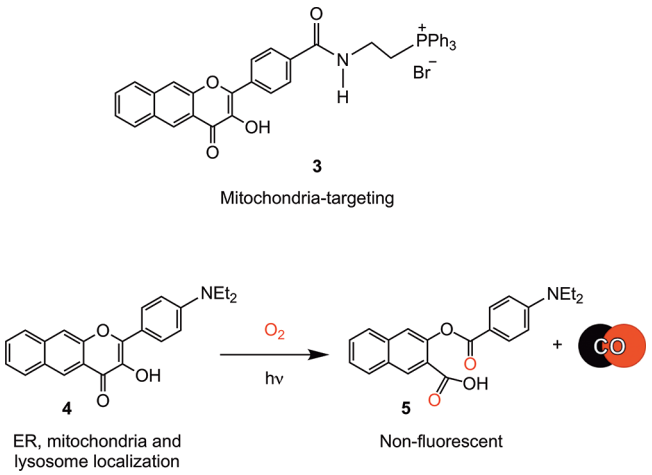

Additional studies are needed to define the relationship between the location of intracellular CO delivery and CO-induced effects. Of particular need are metal-free CO delivery molecules that can be tracked via fluorescence at low micromolar or nanomolar concentrations prior to CO release. In this regard, flavonols containing a *para*-dialkylamino substituent on the B-ring are known for their intense fluorescence.[41] Such molecules have been used as polarity-sensitive probes and fluorescent sensors for biological applications.[42−51] Notably, flavonols containing a $-NPh_2$ moiety have been reported to localize to the ER.[41,50]

We have previously reported the synthesis and light-induced CO release of **4** (Scheme 2) in organic solvents.[23] However, its properties in cells, including its fluorescence trackability and the effects produced when it is used as an intracellular CO delivery molecule, have not been previously investigated. In the studies reported herein, we find that **4** (Scheme 2) is trackable in cells at concentrations as low as 1 μM. This observation sets a new benchmark for the field in terms of a trackable metal-free CO delivery molecule.[52] Confocal microscopy studies indicate **4** localizes to the ER, with additional localization at mitochondria and lysosomes. Although it is nontoxic up to 100 μM in the dark, light-induced CO release from **4** produces significantly enhanced toxicity at low micromolar concentrations relative to that produced by cytosolic **1**. The localization of **4** also leads to significant anti-inflammatory properties at nanomolar concentrations, an effect that is not produced by **1** at similar concentrations. Visible-light-induced CO release enhances the anti-inflammatory effects of both compounds. Overall, the subcellular localization of **4** produces novel outcomes, suggesting the importance of localized CO delivery in producing biological effects.

Both **1** and **4** can be produced in analytically pure form (>95% by HPLC, Figures S1 and S2) via one-pot synthetic procedures followed by precipitation and washing. The pyrone rings from which CO is released in **1** and **4** are structurally similar, with no significant changes due to the presence of the $-NEt_2$ group (Figure S3 and Table S1). The absorption maximum for **4** in DMSO and acetonitrile is ∼445 nm with a molar absorptivity values of ∼32 000−36 000 M^{-1} cm^{-1} (Figure S4). This absorption feature is red-shifted by ∼25 nm versus the absorption maximum of **1**.[23] When illuminated at its absorption maximum either in CH_3CN or DMSO (λ_{ex} = 445 nm), **4** exhibits a broad intense emission at ∼550 nm (Figure S5). The fluorescence quantum yield and lifetime for **4** ($\Phi_{PL=}$ 25.5; 6.1 ns) are similar to those found for **1** ($\Phi_{PL=}$ 34.5; 7.9 ns).[26]

We have previously reported that **4** (Scheme 2) exhibits a clean visible-light-induced CO release (0.96(2) equiv.) in acetonitrile.[23] A similar reaction was identified in d_6-DMSO using ^{1}H NMR (Figure S6). The CO release in this reaction

https://doi.org/10.1021/acsmedchemlett.1c00595
ACS Med. Chem. Lett. 2022, 13, 236−242

was measured as 1.01 ± 0.02 equiv. Both **1** and **4** undergo light-induced (419 nm) CO release in DMEM/F12K media under air as evidenced by loss of their absorption features (Figure S7). The quantum yields for these CO release reactions are similar regardless of solvent (CH_3CN: **1**, 0.7(3)%; **4**, 0.6(1)%; DMSO: **1**, 0.6(3)%;[26] **4**, 0.5(4)%). The quantum yield for CO release from **4** in DMEM/F12K media (10% DMSO) is similar (0.3(1)%). The organic byproducts **2** and **5** (Schemes 1 and 2) generated in the CO release reactions of **1** and **4** (**5**: Figure S8) do not absorb in the visible region. Compound **4** is stable in CH_3CN for greater than four months if the solution is protected from light. Compounds **1** and **4** interact weakly with bovine serum albumin protein (BSA) (TRIS:DMSO (96:4% v:v, pH 7.4, 298 K), with K_a values of 3.2×10^3 M^{-1} (**1**)[53] and 8.1×10^2 M^{-1} (**4**), respectively, and substoichiometric binding (n = 0.66 and 0.54, respectively; Figure S9). In the presence of BSA (40 equiv.), the quantum yields for CO release for **1** and **4** are 0.06(1) and 0.16(1)%, respectively.[53]

Cytoxicity studies of **1** and **4** were performed in human lung epithelial adenocarcinoma cells (A549), normal human lung fibroblast cells (HFL-1), and mouse macrophage cells (RAW264.7). Compound **1** exhibits mild cytotoxicity in all of the tested cell lines, with the following mean IC_{50} values: 83.0 ± 1.2 μM (A549), 65.1 ± 1.8 μM (HFL-1), and 47.7 ± 1.4 μM (RAW 264.7), respectively. Notably, in the dark, **4** is nontoxic in A549 and HFL-1 cells up to 100 μM (Figure 1, Figures S10 and S11, Table S2). The compound exhibits mild toxicity in RAW264.7 cells (IC_{50} = 67.2 ± 2.0 μM, Figure S12).

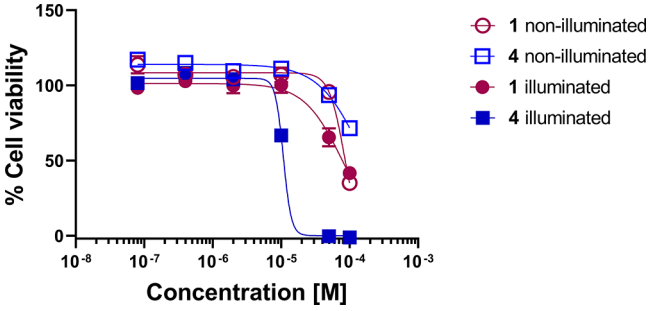

Figure 1. Plot of percent cell viability in A549 cells versus concentration of compounds.

Light-triggered intracellular CO release from **4** produces a significant decrease in IC_{50} values versus those found for **4** without illumination (Figures S10–S12; Table S3). For example, as shown in Figure 1, the increase in toxicity produced upon CO release in A549 cells is characterized by an IC_{50} = 10.7 ± 1.2 μM. This result is notably different than that found for **1**, where IC_{50} values changed only slightly with CO release (Figure 1 and Table S3). Similar CO-induced effects on IC_{50} with **4** were observed in HFL-1 and RAW264.7 cells. The CO release products **2** and **5** were found to be nontoxic (up to 100 μM) in most of the cell lines examined (Table S3). The significant difference in toxicity prior to and following CO release from **4** is a notable feature that has not been identified for other visible-light-induced CO delivery molecules.

Fluorescence microscopy studies of **4** performed in A549 cells at 20× resolution are shown in Figure 2. The emission of **4** is trackable at concentrations as low as 1 μM. In RAW264.7 and HFL-1 cells, **4** is visualizable at concentrations as low as 5

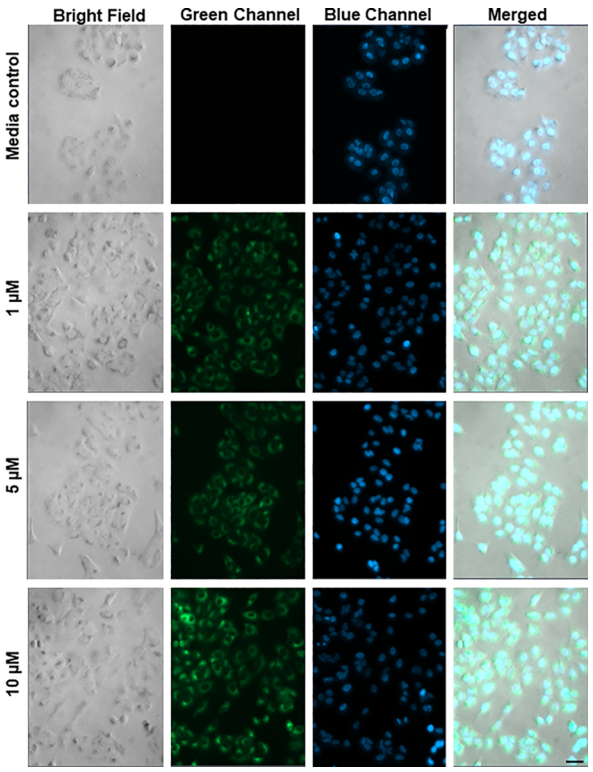

Figure 2. Concentration-dependent fluorescence microscopy images (20×) of A549 cells incubated for 4 h with **4** at 1, 5, and 10 μM followed by washing of the cells prior to imaging. The cells were costained with Hoechst 33342 nuclear dye (blue) to assess cell integrity. Scale bar = 40 μm.

and 1 μM, respectively (Figures S13 and S14). This compound is the most trackable metal-free CO donor reported to date.[51] CO release from **4** can be followed in cells at 1 μM using a CO sensor (Figure S15).[54]

Confocal microscopy studies of **4** in A549 cells showed clustering of the emission (Figure 3), which led us to assess the

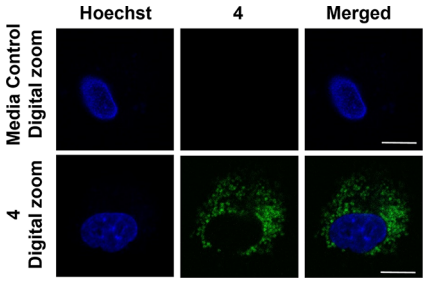

Figure 3. Confocal microscopy images (63×) showing **4** in A549 cells. Row 1, media control. Row 2, cells treated with **4** (1 μM) for 1 h. Images depict the Hoechst nuclear stain (blue), compound **4** (green), and a merge of the two channels. Scale bar = 10 μm.

subcellular localization of the compound via colocalization studies with a series of organelle-specific fluorescent dyes. We first compared the intracellular emission of **4** (Figure 4) to that of ER-Tracker Red.[55] Incubation of A549 cells with **4** at 25 μM for 1 h showed that the compound localizes similarly to the ER-Tracker Red as indicated by the yellow color in the merged image. The overlap between **4** and ER-Tracker Red was determined to be substantial as evidenced by the Pearson's colocalization coefficient, r = 0.88 ± 0.04 (mean ± standard

https://doi.org/10.1021/acsmedchemlett.1c00595
ACS Med. Chem. Lett. 2022, 13, 236–242

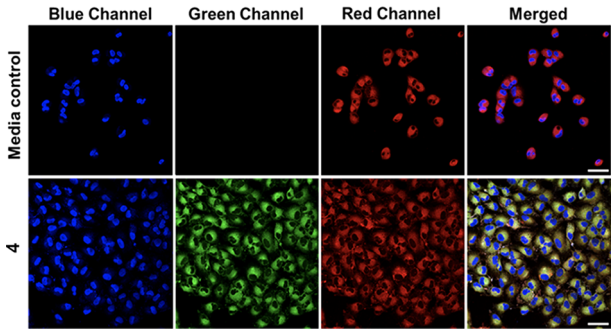

Figure 4. Co-localization of **4** with ER-Tracker Red in A549 cells. Cells were treated with vehicle control (0.4% DMSO) (row 1), or **4** (25 μM, row 2) for 1 h, then counterstained with Hoechst 33342 and ER-Tracker Red. These images depict the Hoechst nuclear stain (blue channel), **4** (green channel), ER-Tracker Red (red channel), and a merge of the three channels. Scale bar = 50 μm.

error of the mean for 27 cells examined individually examined across three separate experiments). Regions of interest and their spatial resolution were evaluated as a line profile over a distance of 20 μm (Figure 5). The congruence of the intensity profiles of **4** and ER-Tracker Red strongly suggest that **4** localizes to the ER.

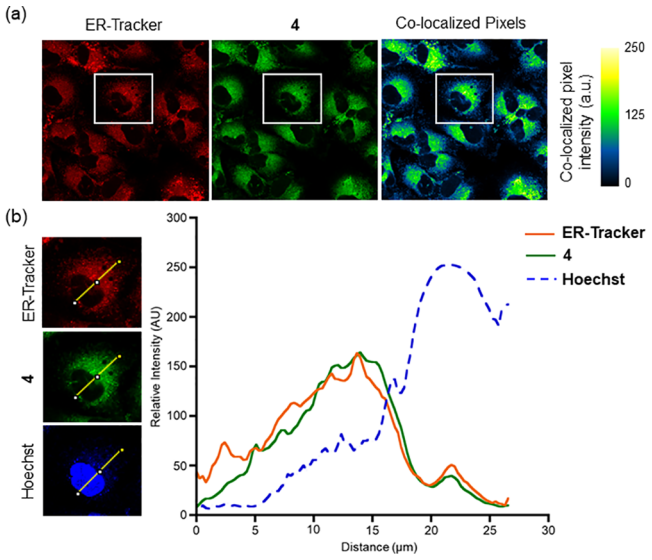

Figure 5. Confocal images of A549 cells costained with **4**, ER-Tracker Red, and Hoechst 33342. (a) Independent and colocalized pixels of **4** and ER-Tracker Red. (b) Overlaid intensity profile of regions of interest in the costained A549 cells as indicated by the white arrows.

Similar confocal analyses were performed using MitoTracker Deep Red (MTR) to probe for mitochondria localization (Figures S16 and S17). Using an experimental approach similar to that described for ER-Tracker Red, a Pearson's colocalization coefficient (r = 0.74 ± 0.09) for MTR was determined. Similarly, colocalization studies with LysoTracker Red produced a Pearson's colocalization coefficient of 0.66 ± 0.08 (Figures S18 and S19).

The identification of subcellular localization to the ER, mitochondria, and lysosomes has been observed with other fluorophores.[56,57] However, to the best of our knowledge, **4** is the first CO delivery molecule to exhibit localization to the ER, a network of membranous tubules with embedded transmembrane proteins, including the CO-generating HO-1.[13] The anti-inflammatory and antiapoptotic properties of CO may be important toward mitigating ER stress associated with vascular diseases.[58] To date, a small number of studies focused on examining the effect of CO delivery on ER stress have been reported.[59,60] These were performed using CORM-2, a Ru(II)-containing spontaneous CO delivery molecule with no reported subcellular localization properties. Recent identification of Ru(II) impacting the results of other biological studies involving CORM-2[61] suggests that new CO delivery tools such as **4** should be considered to probe the impact of CO on ER stress.

Compound **4** is the second extended CO-releasing flavonol to show mitochondrial localization, with **3** (Scheme 2(top)) being the other example.[40] The differences in toxicity between **3** and **4** in the presence and absence of CO release are notable. In the absence of CO release, **3** produces significant toxicity in A549 cells (IC_{50} = 14.1 ± 2.7 μM), whereas **4** is nontoxic up to 100 μM. Whereas CO release from **3** produces a minimal increase in toxicity (IC_{50} = 4.6 ± 3.6 μM), CO release from **4** results in notably increased toxicity (IC_{50} = 10.7 ± 1.2 μM; Figure 6). The enhanced toxicity induced via CO release from

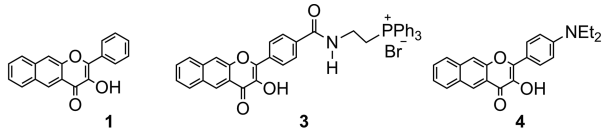

A549 cells:	1 cytosolic	3 mitochondrial localization	4 ER, mitochondrial and lysozome localization
IC_{50} (μM)	83.0 +/- 1.2	14.1 +/- 2.7	> 100
IC_{50} (μM; with CO relase)	77.2 +/- 3.2	4.6 +/- 3.6	10.7 +/- 1.2

Figure 6. Comparison of IC_{50} values of extended flavonols in A549 cells.

4 versus cytosolic **1** strongly suggests that differences in subcellular localization modulate CO-induced effects. This is an area in significant need of advancement, as little data currently exist regarding the effects of localized CO release.

The lysosome localization of **4** is not unexpected as dialkylamino-appended fluorophores for lysosome targeting have been previously reported.[62] This is the first CO-releasing molecule to exhibit lysosome localization.

We next determined how CO release from **4** attenuates LPS-induced inflammation by suppressing the production of TNF-α. We have performed similar experiments using **1** and a sulfonated analog.[63] Experiments with **4** were independently performed in the dark and under illumination conditions. As shown in Figure 7, compound **4** exhibits significant TNF-α suppression at 40 nM in the absence of CO release. This anti-inflammatory effect is the most potent of the extended flavonols that we have examined thus far, suggesting an important influence resulting from subcellular localization. With CO release, the anti-inflammatory effects of **4** at nanomolar concentrations are enhanced, as evidenced by greater TNF-α suppression (Figure 7). We note that the concentration dependent increase in TNF-α suppression is attenuated for **4** as compared to that of **1**, which may be a result of its enhanced effectiveness at low concentrations. Previously reported CORMs, such as CORM-3 and a BSA-$Ru(CO)_2$ conjugate, reduce TNF-α expression in RAW264.7

https://doi.org/10.1021/acsmedchemlett.1c00595
ACS Med. Chem. Lett. 2022, 13, 236−242

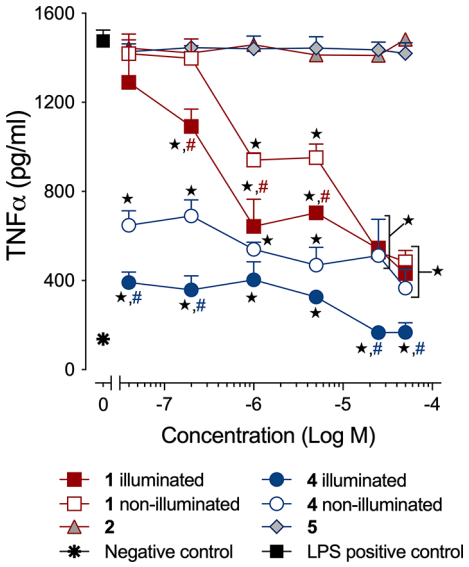

Figure 7. Anti-inflammatory effects of **1** and **4** in RAW 264.7 cells under dark or light conditions. The results are presented as the mean ± SEM from three independent experiments. ★, $p < 0.01$ compared to LPS positive control; #, $p < 0.05$ compared to corresponding nonilluminated treatment with red for **1** and blue for **4**.

murine macrophages at concentrations of 10 and 4.5 μM, respectively.[64,65] Spontaneous metal-free CO releasing molecules produce anti-inflammatory effects at similar low micromolar concentrations.[66] Suppression of TNF-α by nanomolar concentrations of **4** with CO release is most similar to that produced via CO release from a BSA-delivered quinolone, which cannot be trackable in cells because of low fluorescence intensity.[26]

Highly trackable, organelle-targeted metal-free CO donors remain rare.[67] The low micromolar fluorescence trackability of **4** is notable, making it a novel probe to evaluate the effects of localized intracellular CO release. The subcellular localization of **4** to the ER, mitochondria, and lysosomes produces significant CO-induced toxicity effects that are distinct from analogs with different localization properties. The observed difference in toxicity provides evidence that the intracellular localization of the CO release influences the magnitude of its biological effects. Further investigations are underway using a series of amino-appended flavonols to examine subcellular localization effects on CO-induced toxicity and anti-inflammatory effects. Overall, **4** represents a prototype on which to base the development of additional highly fluorescent, localized, and triggered CO delivery molecules to define how the site of CO delivery impacts it biological effects. We note that because of the limited number of hydroxyl substituents in **4** versus naturally occurring flavonols (e.g., quercetin), this compound is expected to have less biological promiscuity and does not register warnings as a PAINS substance.[68] Overall, the results outlined here provide evidence that **4** is a novel compound for localized CO delivery, which might also be pursued using materials-based approaches.[34−38]

■ ASSOCIATED CONTENT

Supporting Information

The Supporting Information is available free of charge at https://pubs.acs.org/doi/10.1021/acsmedchemlett.1c00595.

Experimental procedures as well as spectroscopic, cell viability, and confocal imaging data (PDF)

Crystallographic information file for **4** (CIF)

■ AUTHOR INFORMATION

Corresponding Author

Lisa M. Berreau − *Department of Chemistry and Biochemistry, Utah State University, Logan, Utah 84322-0300, United States;* orcid.org/0000-0001-9599-5239; Email: lisa.berreau@usu.edu

Authors

Livia S. Lazarus − *Department of Chemistry and Biochemistry, Utah State University, Logan, Utah 84322-0300, United States;* orcid.org/0000-0002-3001-3190

C. Taylor Dederich − *Department of Chemistry and Biochemistry, Utah State University, Logan, Utah 84322-0300, United States;* orcid.org/0000-0002-8245-7914

Stephen N. Anderson − *Department of Chemistry and Biochemistry, Utah State University, Logan, Utah 84322-0300, United States*

Abby D. Benninghoff − *Department of Animal, Dairy and Veterinary Sciences, Utah State University, Logan, Utah 84322-4815, United States;* orcid.org/0000-0002-7993-0117

Complete contact information is available at: https://pubs.acs.org/10.1021/acsmedchemlett.1c00595

Author Contributions

L.M.B., L.S.L., C.T.D., and A.B.D. designed the research. L.S.L., C.T.D., and S.N.A. performed the experiments. L.M.B., L.S.L., C.T.D., S.N.A., and A.B.D. performed the data analysis. The manuscript was written by L.M.B., L.S.L., C.T.D., and A.D.B.. All authors approved the final version of the manuscript.

Notes

The authors declare no competing financial interest.

■ ACKNOWLEDGMENTS

We thank the NIH (R15GM124596 to L.M.B. and A.D.B.), the Utah Agricultural Experiment Station (project UTA-1456 to A.D.B.), the National Science Foundation (CHE-1429195 for Brüker Avance III HD 500 MHz NMR; CHE-1828764 for Rigaku Benchtop XtaLAB Mini II X-ray diffractometer), the American Heart Association (grant 18PRE34030099 to L.S.L.), and the USU Office of Research (PDRF Fellowship to L.S.L.) for financial support. We thank Suliman Ayad (Florida State University) for performing fluorescence quantum yield and lifetime studies of **4**.

■ ABBREVIATIONS

DMEM, Dulbecco's modified Eagle medium; IC_{50}, half minimum inhibitory concentration; LPS, lipopolysaccharide; MTR, MitoTracker Deep Red; TNF, tumor necrosis factor; SEM, standard error of the mean; PAINS, pan assay interference compounds

■ REFERENCES

(1) Hopper, C. P.; Zambrana, P. N.; Goebel, U.; Wollborn, J. A Brief History of Carbon Monoxide and its Therapeutic Origin. *Nitric Oxide* **2021**, *111−112*, 45−63.

(2) Motterlini, R.; Foresti, R. Biological Signaling by Carbon Monoxide and Carbon Monoxide-releasing Molecules. *Am. J. Physiol. Cell. Physiol.* **2017**, *312*, C302−C313.
(3) Ryter, S. W.; Alam, J.; Choi, A. M. K. Heme Oxygenase-1/Carbon Monoxide: From Basic Science to Therapeutic Applications. *Physiol. Rev.* **2006**, *86*, 583−650.
(4) Tenhunen, R.; Marver, H. S.; Schmid, R. The Enzymatic Conversion of Heme to Bilirubin by Microsomal Heme Oxygenase. *Proc. Natl. Acad. Sci. U.S.A.* **1968**, *61*, 748−755.
(5) Tenhunen, R.; Marver, H. S.; Schmid, R. Microsomal Heme Oxygenase. Characterization of the Enzyme. *J. Biol. Chem.* **1969**, *244*, 6388−6394.
(6) Otterbein, L. E.; Choi, A. M. Heme Oxygenase: Colors of Defense against Cellular Stress. *Am. J. Physiol. Lung Cell Mol. Physiol.* **2000**, *279*, L1029−L1037.
(7) Motterlini, R.; Otterbein, L. E. The Therapeutic Potential of Carbon Monoxide. *Nat. Rev. Drug Discovery* **2010**, *9*, 728−743.
(8) Cheng, J.; Gan, G.; Shen, Z.; Gao, L.; Zhang, G.; Hu, J. Red-light-Triggered Intracellular Carbon Monoxide Release Enables Selective Eradication of MRSA Infection. *Angew. Chem., Int. Ed.* **2021**, *60*, 13513−13520.
(9) Kourti, M.; Jiang, W. G.; Cai, J. Aspects of Carbon Monoxide in Form of CO-releasing Molecules Used in Cancer Treatment: More Light on the Way. *Oxid. Med. Cell. Longev.* **2017**, *2017*, 9326454.
(10) Goebel, U.; Wollborn, J. Carbon Monoxide in Intensive Care Medicine - Time to Start the Therapeutic Application?! *Intensive Care Med. Exp.* **2020**, *8*, 2.
(11) Yan, H.; Du, J.; Zhu, S.; Nie, G.; Zhang, H.; Gu, Z.; Zhao, Y. Emerging Delivery Strategies of Carbon Monoxide for Therapeutic Applications: From CO Gas to CO Releasing Nanomaterials. *Small* **2019**, *15*, 1904382.
(12) Gottlieb, Y.; Truman, M.; Cohen, L. A.; Leichtmann-Bardoogo, Y.; Meyron-Holtz, E. G. Endoplasmic Reticulum Anchored Heme-Oxygenase 1 Faces the Cytosol. *Haematologica* **2012**, *97*, 1489−1493.
(13) Dunn, L. L.; Midwinter, R. G.; Ni, J.; Hamid, H. A.; Parish, C. R.; Stocker, R. New Insights into Intracellular Locations and Functions of Heme Oxygenase-1. *Antioxid. Redox Signal* **2014**, *20*, 1723−1742.
(14) Motterlini, R. Carbon Monoxide-Releasing Molecules (CO-RMs): Vasodialatory, Anti-Ischaemic, and Anti-inflammatory Activities. *Biochem. Soc. Trans.* **2007**, *35*, 1142−1146.
(15) Mann, B. E. CO-Releasing Molecules: A Personal View. *Organometallics* **2012**, *31*, 5728−5735.
(16) Southam, H. M.; Smith, T. W.; Lyon, R. L.; Liao, C.; Trevitt, C. R.; Middlemiss, L. A.; Cox, F. L.; Chapman, J. A.; El-Khamisy, S. F.; Hippler, M.; Williamson, M. P.; Henderson, P. J. F.; Poole, R. K. A Thiol Reactive Ru(II) Ion, Not CO Release, Underlies the Potent Antimicrobial and Cytotoxic Properties of CO-releasing Molecule-3. *Redox Biol.* **2018**, *18*, 114−123.
(17) Stucki, D.; Krahl, H.; Walter, M.; Steinhausen, J.; Hommel, K.; Brenneisen, P.; Stahl, W. Effects of Frequently Applied Carbon Monoxide Releasing Molecules (CORMs) in Typical CO-Sensitive Model Systems - A Comparative *In Vitro* Study. *Arch. Biochem. Biophys.* **2020**, *687*, 108383.
(18) Yuan, Z.; Yang, X.; Ye, Y.; Tripathi, R.; Wang, B. Chemical Reactivities of Two Widely Used Ruthenium-Based CO-Releasing Molecules with a Range of Biologically Important Reagents and Molecules. *Anal. Chem.* **2021**, *93*, 5317−5326.
(19) Motterlini, R.; Clark, J. E.; Foresti, R.; Sarathchandra, P.; Mann, B. E.; Green, C. J. Carbon Monoxide-Releasing Molecules: Characterization of Biochemical and Vascular Activities. *Circ. Res.* **2002**, *90*, E17−E24.
(20) Foresti, R.; Hammad, J.; Clark, J. E.; Johnson, T. R.; Mann, B. E.; Friebe, A.; Green, C. J.; Motterlini, R. Vasoactive Properties of CORM-3, a Novel Water-Soluble Carbon Monoxide-Releasing Molecule. *Br. J. Pharmacol.* **2004**, *142*, 453−460.
(21) Antony, L. A. P.; Slanina, T.; Sebej, P.; Solomek, T.; Klan, P. Fluorescein Analogue Xanthene-9-Carboxylic Acid: A Transition-Metal-Free CO Releasing Molecule Activated by Green Light. *Org. Lett.* **2013**, *15*, 4552−4555.
(22) Peng, P.; Wang, C.; Shi, Z.; Johns, V. K.; Ma, L.; Oyer, J.; Copik, A.; Igarashi, R.; Liao, Y. Visible-Light Activatable Organic CO-Releasing Molecules (PhotoCORMs) That Simultaneously Generate Fluorophores. *Org. Biomol. Chem.* **2013**, *11*, 6671−6674.
(23) Anderson, S. N.; Richards, J. M.; Esquer, H. J.; Benninghoff, A. D.; Arif, A. M.; Berreau, L. M. A Structurally-Tunable 3-Hydroxyflavone Motif for Visible Light-Induced Carbon Monoxide-Releasing Molecules (CORMs). *ChemistryOpen* **2015**, *4*, 590−594.
(24) Palao, E.; Slanina, T.; Muchova, L.; Solomek, T.; Vitek, L.; Klan, P. Transition-Metal-Free CO-Releasing BODIPY Derivatives Activatable by Visible to NIR Light as Promising Bioactive Molecules. *J. Am. Chem. Soc.* **2016**, *138*, 126−133.
(25) Abeyrathna, N.; Washington, K.; Bashur, C.; Liao, Y. Nonmetallic Carbon Monoxide Releasing Molecules (CORMs). *Org. Biomol. Chem.* **2017**, *15*, 8692−8699.
(26) Popova, M.; Lazarus, L. S.; Ayad, S.; Benninghoff, A. D.; Berreau, L. M. Visible-Light-Activated Quinolone Carbon-Monoxide-Releasing Molecule: Prodrug and Albumin-Assisted Delivery Enables Anticancer and Potent Anti-Inflammatory Effects. *J. Am. Chem. Soc.* **2018**, *140*, 9721−9729.
(27) Ji, X.; Wang, B. Strategies toward Organic Carbon Monoxide Prodrugs. *Acc. Chem. Res.* **2018**, *51*, 1377−1385.
(28) Feng, W.; Feng, S.; Feng, G. CO Release with Ratiometric Fluorescence Changes: A Promising Visible-Light-Triggered Metal-Free CO-Releasing Molecule. *Chem. Commun.* **2019**, *55*, 8987−8990.
(29) Wang, X.; Chen, X.; Song, L.; Zhou, R.; Luan, S. An Enzyme-Responsive and Photoactivatable Carbon-Monoxide Releasing Molecule for Bacterial Infection Theranostics. *J. Mater. Chem. B* **2020**, *8*, 9325−9334.
(30) Stackova, L.; Russo, M.; Muchova, L.; Orel, V.; Vitek, L.; Stacko, P.; Klan, P. Cyanine-Flavonol Hybrids for Near-Infrared Light-Activated Delivery of Carbon Monoxide. *Chemistry* **2020**, *26*, 13184−13190.
(31) Lazarus, L. S.; Benninghoff, A. D.; Berreau, L. M. Development of Triggerable, Trackable, and Targetable Carbon Monoxide Releasing Molecules. *Acc. Chem. Res.* **2020**, *53*, 2273−2285.
(32) Thiang Brian Kueh, J.; Seifert-Simpson, J. M.; Thwaite, S. H.; Rodgers, G. D.; Harrison, J. C.; Sammut, I. A.; Larsen, D. S. Studies Towards Non-Toxic, Water-Soluble, Vasoactive Norbornene Organic Carbon Monoxide Releasing Molecules. *Asian J. Org. Chem.* **2020**, *9*, 2127−2135.
(33) Pan, Z.; Chittavong, V.; Li, W.; Zhang, J.; Ji, K.; Zhu, M.; Ji, X.; Wang, B. Organic CO Prodrugs: Structure-CO Release Rate Relationship Studies. *Chem.—Eur. J.* **2017**, *23*, 9838−9845.
(34) Cheng, J.; Zheng, B.; Cheng, S.; Zhang, G.; Hu, J. Metal-free Carbon Monoxide-Releasing Micelles Undergo Tandem Photochemical Reactions for Cutaneous Wound Healing. *Chem. Sci.* **2020**, *11*, 4499−4507.
(35) Liu, C.; Du, Z.; Ma, M.; Sun, Y.; Ren, J.; Qu, X. Carbon Monoxide Controllable Targeted Gas Therapy for Synergistic Anti-inflammation. *iScience* **2020**, *23*, 101483.
(36) Zhang, M.; Cheng, J.; Huang, X.; Zhang, G.; Ding, S.; Hu, J.; Qiao, R. Photo-Degradable Micelles Capable of Releasing Carbon Monoxide under Visible Light Irradiation. *Macromol. Rapid Commun.* **2020**, *41*, 2000323.
(37) Tao, S.; Cheng, J.; Su, G.; Li, D.; Shen, Z.; Tao, F.; You, T.; Hu, J. Breathing Micelles for Combinatorial Treatment of Rheumatoid Arthritis. *Angew. Chem., Int. Ed.* **2020**, *59*, 21864−21869.
(38) Sun, P.; Jia, L.; Hai, J.; Lu, S.; Chen, F.; Liang, K.; Sun, S.; Liu, H.; Fu, X.; Zhu, Y.; Wang, B. Tumor Microenvironment -"AND" Near-Infrared Light-Activated Coordination Polymer Nanoprodrug for On-Demand CO-Sensitized Synergistic Cancer Therapy. *Adv. Healthc. Mater.* **2021**, *10*, 2001728.
(39) Zheng, Y.; Ji, X.; Yu, B.; Ji, K.; Gallo, D.; Csizmadia, E.; Zhu, M.; Choudhury, M. R.; De La Cruz, L. K. C.; Chittavong, V.; Pan, Z.; Yuan, Z.; Otterbein, L. E.; Wang, B. Enrichment-Triggered Prodrug

https://doi.org/10.1021/acsmedchemlett.1c00595
ACS Med. Chem. Lett. 2022, 13, 236−242

Activation Demonstrated through Mitochondria-Targeted Delivery of Doxorubicin and Carbon Monoxide. *Nat. Chem.* **2018**, *10*, 787−794.
(40) Lazarus, L. S.; Esquer, H. J.; Anderson, S. N.; Berreau, L. M.; Benninghoff, A. D. Mitochondrial-localized versus Cytosolic Intracellular CO-releasing Organic PhotoCORMs: Evaluation of CO Effects using Bioenergetics. *ACS Chem. Biol.* **2018**, *13*, 2220−2228.
(41) Guo, L.; Tian, M.; Zhang, Z.; Lu, Q.; Liu, Z.; Niu, G.; Yu, X. Simultaneous Two-Color Visualization of Lipid Droplets and Endoplasmic Reticulum and Their Interplay by Single Fluorescent Probes in Lambda Mode. *J. Am. Chem. Soc.* **2021**, *143*, 3169−3179.
(42) Sytnik, A.; Gormin, D.; Kasha, M. Interplay between Excited-State Intramolecular Proton Transfer and Charge Transfer in Flavonols and Their Use as Protein-binding-site Fluorescence Probes. *Proc. Natl. Acad. Sci. U.S.A.* **1994**, *91*, 11968−11972.
(43) Klymchenko, A. S. Solvatochromic and Fluorogenic Dyes as Environment-sensitive Probes: Design and Biological Applications. *Acc. Chem. Res.* **2017**, *50*, 366−375.
(44) Zhu, K.; Lv, T.; Qin, T.; Huang, Y.; Wang, L.; Liu, B. A Flavonoid-based Fluorescent Probe Enables the Accurate Quantification of Human Serum Albumin by Minimizing the Interference from Blood Lipids. *Chem. Commun.* **2019**, *55*, 13983−13986.
(45) Tian, M.; Sun, J.; Tang, W.; Dong, B.; Lin, W. Discriminating Live and Dead Cells in Dual-color Mode with a Two-photon Fluorescent Probe Based on ESIPT Mechanism. *Anal. Chem.* **2018**, *90*, 998−1005.
(46) Wu, Q.; Wang, K.; Wang, Z.; Sun, Y.; Cao, D.; Liu, Z.; Guan, R.; Zhao, S.; Yu, X. Two 3-Hydroxyflavone Derivatives as Two-photon Fluorescence Turn-on Chemosensors for Cysteine and Homocysteine in Cells. *Talanta* **2018**, *181*, 118−124.
(47) Liu, B.; Pang, Y.; Bouhenni, R.; Duah, E.; Paruchuri, S.; McDonald, L. A Step Toward Simplified Detection of Serum Albumin on SDS-PAGE Using an Environment-Sensitive Flavone Sensor. *Chem. Commun.* **2015**, *51*, 11060−11063.
(48) Liu, Y.; Yu, D.; Ding, S.; Xiao, Q.; Guo, J.; Feng, G. Rapid and Ratiometric Fluorescent Detection of Cysteine with High Selectivity and Sensitivity by a Simple and Readily Available Probe. *ACS Appl. Mater. Interfaces* **2014**, *6*, 17543−17550.
(49) Lan, M.; Wu, J.; Liu, W.; Zhang, H.; Zhang, W.; Zhuang, X.; Wang, P. Highly Sensitive Fluorescent Probe for Thiols Based on Combination of PET and EISPT Mechanisms. *Sens. Actuators B: Chem.* **2011**, *156*, 332−337.
(50) McDonald, L.; Liu, B.; Taraboletti, A.; Whiddon, K.; Shriver, L. P.; Konopka, M.; Liu, Q.; Pang, Y. Fluorescent Flavonoids for Endoplasmic Reticulum Cell Imaging. *J. Mater. Chem. B* **2016**, *4*, 7902−7908.
(51) Ormson, S. M.; Brown, R. G.; Vollmer, F.; Rettig, W. Switching between Charge- and Proton-transfer Emission in the Excited State of a Substituted 3-Hydroxyflavone. *J. Photochem. Photobiol., A* **1994**, *81*, 65−72.
(52) Soboleva, T.; Berreau, L. M. Tracking CO Release in Cells via the Luminescence of Donor Molecules and/or Their Byproducts. *Isr. J. Chem.* **2019**, *59*, 339−350.
(53) Popova, M.; Soboleva, T.; Arif, A. M.; Berreau, L. M. Properties of a Flavonol-based PhotoCORM in Aqueous Buffered solutions: Influence of Metal Ions, surfactants and Proteins on Visible Light-induced CO Release. *RSC Adv.* **2017**, *7*, 21997−22007.
(54) Liu, K.; Kong, X.; Ma, Y.; Lin, W. Rational Design of a Robust Fluorescent Probe for the Detection of Endogenous Carbon Monoxide in Living Zebrafish Embryos and Mouse Tissue. *Angew. Chem. Int. Ed* **2017**, *56*, 13489−13492.
(55) Shim, S.-H.; Xia, C.; Zhong, G.; Babcock, H. P.; Vaughan, J. C.; Huang, B.; Wang, X.; Xu, C.; Bi, G.-Q.; Zhuang, X. Super-resolution Fluorescence Imaging of Organelles in Live Cells with Photoswitchable Membrane Probes. *Proc. Natl. Acad. Sci. U. S. A.* **2012**, *109*, 13978−13983.
(56) Wang, Y.-N.; Zhang, X.-Q.; Qiu, L.-H.; Sun, R.; Xu, Y.-J.; Ge, J.-F. Viscosity Sensitive Endoplasmic Reticulum Fluorescent Probes based on Oxazolopyridinium. *J. Mater. Chem. B* **2021**, *9*, 5664−5669.
(57) Li, S.-J.; Zhou, D.-Y.; Li, Y.; Liu, H.-W.; Wu, P.; Ou-Yang, J.; Jiang, W. J.; Li, C. Y. Efficient Two-Photon Fluorescent Probe for Imaging of Nitric Oxide during Endoplasmic Reticulum Stress. *ACS Sens.* **2018**, *3*, 2311−2319.
(58) Gáll, T.; Balla, G.; Balla, J. Heme, Heme Oxygenase, and Endoplasmic Reticulum Stress - A New Insight into the Pathophysiology of Vascular Diseases. *Int. J. Mol. Sci.* **2019**, *20*, 3675.
(59) Chung, J.; Shin, D.-Y.; Zheng, M.; Joe, Y.; Pae, H.-O.; Ryter, S. W.; Chung, H.-T. Carbon Monoxide, A Reaction Product of Heme Oxygenase-1, Suppresses the Expression of C-reactive Protein by Endoplasmic Reticulum Stress through Modulation of the Unfolded Protein Response. *Mol. Immunol.* **2011**, *48*, 1793−1799.
(60) Zheng, M.; Zhang, Q.; Joe, Y.; Kim, S.-K.; Uddin, J.; Rhew, H.; Kim, T.; Ryter, S.W.; Chung, H. T. Carbon-monoxide Releasing Molecules Reverse Leptin Resistance Induced by Endoplasmic Reticulum Stress. *Am. J. Physiol. Endocrinol. Metab.* **2013**, *304*, E780−788.
(61) Southam, H. M.; Williamson, M. P.; Chapman, J. A.; Lyon, R. L.; Trevitt, C. R.; Henderson, P. J. F.; Poole, R. K. 'Carbon-Monoxide-Releasing Molecule-2 (CORM-2)' Is a Misnomer: Ruthenium Toxicity, Not CO Release, Accounts for its Antimicrobial Effects. *Antioxidants* **2021**, *10*, 915.
(62) Yu, H.; Guo, Y.; Zhu, W.; Havener, K.; Zheng, X. Recent Advances in 1,8-Naphthalimide-based Small-Molecule Fluorescent Probes for Organelles Imaging and Tracking in Living Cells. *Coord. Chem. Rev.* **2021**, *444*, 214019.
(63) Lazarus, L. S.; Simons, C. R.; Arcidiacono, A.; Benninghoff, A. D.; Berreau, L. M. Extracellular vs Intracellular Delivery of CO: Does it Matter for a Stable, Diffusible Gasotransmitter? *J. Med. Chem.* **2019**, *62*, 9990−9995.
(64) Chaves-Ferreira, M.; Albuquerque, I. S.; Matak-Vinkovic, D.; Coelho, A. C.; Carvalho, S. M.; Saraiva, L. M.; Romao, C. C.; Bernardes, G. J. L. Spontaneous CO Release from $Ru^{II}(CO)_2$-Protein Complexes in Aqueous Solution, Cells, and Mice. *Angew. Chem., Int. Ed.* **2015**, *54*, 1172−1175.
(65) Sawle, P.; Foresti, R.; Mann, B. E.; Johnson, T. R.; Green, C. J.; Motterlini, R. Carbon Monoxide-releasing Molecules (CO-RMs) Attenuate the Inflammatory Response Elicited by Lipopolysaccharide in RAW264.7 Murine Macrophages. *Br. J. Pharmacol.* **2005**, *145*, 800−810.
(66) Ji, X.; Ji, K.; Chittavong, V.; Yu, B.; Pan, Z.; Wang, B. An Esterase-activated Click and Release Approach to Metal-free CO-prodrugs. *Chem. Commun.* **2017**, *53*, 8296−8299.
(67) Choi, N.-E.; Lee, J.-Y.; Park, E.-C.; Lee, J.-H.; Lee, J. Recent Advances in Organelle-targeted Fluorescent Probes. *Molecules* **2021**, *26*, 217.
(68) Baell, J. B.; Holloway, G. A. New Substructure Filters for Removal of Pan Assay Interference Compounds (PAINS) from Screening Libraries and for their Exclusion in Bioassays. *J. Med. Chem.* **2010**, *53*, 2719−2740.

https://doi.org/10.1021/acsmedchemlett.1c00595
ACS Med. Chem. Lett. 2022, 13, 236−242